Neuropilin-1 promotes primary liver cancer progression by potentiating the activity of hepatic stellate cells

ZHI-CHAO XU*, HAO-XIN SHEN*, CHEN CHEN, LI MA, WEN-ZHI LI, LIN WANG and ZHI-MIN GENG

Department of Hepatobiliary Surgery, First Affiliated Hospital of Xi'an Jiaotong University, Xi'an, Shaanxi 710061, P.R. China

Received December 22, 2015; Accepted July 20, 2017

DOI: 10.3892/ol.2017.7541

Abstract. As a co-receptor for a variety of cytokines, neuropilin-1 (NRP-1) is detectable in primary liver cancer (PLC) cells. Previous studies determined that silencing of NRP-1 expression attenuated the proliferation, migration and invasion of PLC cells. An increasing number of studies have highlighted the crucial role of the tumor microenvironment in the pathogenesis of cancer. Hepatic stellate cells (HSCs) are one of the major interstitial cell types present in the liver tumor microenvironment, and can promote the proliferation, migration and invasion of PLC cells. It remains unknown whether NRP-1 can promote PLC progression by potentiating the activity of HSCs. In the present study, the expression of NRP-1, and its co-expression with platelet-derived growth factor receptor-β, in HSCs was detected via immunofluorescence. LX2 HSCs were transfected with NRP-1 short hairpin RNA lentiviral vectors and their proliferation was observed. The proliferation, migration and invasion of HepG2 cells co-cultured with LX2 cells were also observed. Finally, LX2 and HepG2 cells were co-injected into nude mice as subcutaneous xenografts, and the tumor growth and α-smooth muscle actin expression levels were observed. NRP-1 knockdown attenuated LX2 cell activation, with concomitant downregulation of HepG2 cell proliferation, migration and invasion ($P<0.05$). Thus, silencing of NRP-1 expression may inhibit the activation of HSCs, as well as the proliferation, migration and invasion of PLC cells. The mechanism underlying the inhibition of PLC cell progression is possibly mediated by the inhibition of HSC activation, reduction of transforming growth factor-β1 levels in the conditioned medium and downregulation of extracellular signal-related kinase activity in PLC cells. Thus, NRP-1 could be regarded as a potential gene therapy target for PLC.

Correspondence to: Dr Zhi-Min Geng, Department of Hepatobiliary Surgery, First Affiliated Hospital of Xi'an Jiaotong University, 277 West Yanta Road, Xi'an, Shaanxi 710061, P.R. China
E-mail: gengzhimin@mail.xjtu.edu.cn

*Contributed equally

Key words: neuropilin-1, hepatic stellate cells, primary liver cancer, tumor microenvironment

Introduction

Primary liver cancer (PLC) is one of the most fatal types of cancer in humans with a rising incidence worldwide. It accounts for 70-90% of the total liver cancer burden and is the third most common cause of cancer-associated mortality globally (1). Long-term prognosis of PLC remains poor, with the majority of patients succumbing to disease due to recurrence. Therefore, understanding the pathogenesis of primary PLC is crucial for improving the efficacy of current treatment strategies.

The liver tumor microenvironment is an essential contributor to PLC initiation and progression. It has been demonstrated that various stromal cell types are recruited to neoplasms, where they are activated and substantially promote the proliferation, invasion and metastatic potential of cancer cells (2,3). Hepatic stellate cells (HSCs) belong to one of the most important stromal cell types in the liver tumor environment. Numerous prior studies have revealed that culturing hepatocytes and LX2 cells (a spontaneous immortalized human HSC cell line) results in bidirectional cross-talk, with LX2 cells promoting PLC proliferation and migration, thus inducing an inflammatory reaction (4,5). Simultaneous *in vivo* subcutaneous implantation of human HSCs and PLC cells in nude mice promotes tumor growth, invasiveness and inhibits necrosis (6).

Neuropilin-1 (NRP-1) is a transmembrane receptor for class 3 semaphorins (7) and vascular endothelial growth factor isoforms (8). It is expressed in a wide range of tissues and mediates diverse cellular functions, including migration, adhesion, proliferation and apoptosis (9,10). Recently, NRP-1 has been implicated in HSC activation and cirrhosis progression (11). However, the effect of HSCs on PLC cells following NRP-1 expression silencing remains unclear. The present study demonstrated that silencing NRP-1 expression of HSCs may inhibit the activation of HSCs, as well as attenuate the malignant progression of PLC cells *in vitro* and *in vivo*.

Materials and methods

Cell lines and culture. The LX2 human HSCs were provided by the American Type Culture Collection (Manassas, VA, USA). HepG2 human hepatoblastoma cells were provided by the Translation Medicine Center of Xi'an Jiaotong University (Xi'an, China). LX2 and HepG2 cells were cultured in

Dulbecco's modified Eagle's medium (DMEM; HyClone; GE Healthcare, Chicago, IL, USA) supplemented with 10% fetal bovine serum (FBS; MP Biomedicals, Solon, OH, USA) and 1% streptomycin/penicillin (100 IU/ml; Gibco; Thermo Fisher Scientific, Inc., Waltham, MA, USA) with 5% CO_2 at 37˚C for 24 h in imunofluorescence staining, ELISA, migration and invasion assays, 48 h in western blot analysis, 72 h in lentivirus transfection, MTT assay and *in vivo* experiments.

Expression constructs and transfection. Lentivirus pGCSIL-RFPshNRP1 was constructed in preliminary experiments (12). LX2 cells were transfected with non-targeting (NT) short hairpin (sh)RNA lentiviruses (NT shRNA) or NRP-1 shRNA lentiviruses to yield stable NRP-1 knockdown LX2 cells (LX2-NRP-1 shRNA) and stable control LX2 cells (LX2-NT shRNA). Transfection of LX2 with viral particles was performed by incubating cells with viral supernatant (25%) supplemented with polybrene (5 μg/ml; Santa Cruz Biotechnology, Inc., Dallas, TX, USA) overnight at 37˚C. Following 48 h, the cells were harvested for further experiments. Lentiviral transduction efficiency was determined by western blot analysis. In order to prepare the conditioned medium (CM), the cells in each group were washed twice with serum-free DMEM one day following seeding into T25 flasks ($2x10^6$ cells), and subsequently incubated for 24 h with serum-free DMEM at 37˚C.

MTT assay. For the MTT assay, stable NRP-1 knockdown LX2 and HepG2 cells were used. Briefly, cells were seeded into 96-well plates at $1x10^4$ cells/well and stained with 100 μl MTT (0.5 mg/ml; BioTime, Inc., Alameda, CA, USA) for 4 h at 37˚C. Subsequently, the culture medium was removed and 150 μl dimethyl sulfoxide (Sigma-Aldrich; Merck KGaA, Darmstadt, Germany) was added to each well. The absorbance was evaluated at 490 nm. Experiments were performed in triplicate and repeated three times with consistent results.

Migration and invasion assays. In order to assess the paracrine effects of HSCs on tumor invasion and migration, LX2 cells with or without NRP-1 knockdown were serum starved and CM were collected. The Transwell chambers (pore size, 8.0 μm; EMD Millipore, Billerica, MA, USA) without (for the migration assay) or with Matrigel (for the invasion assay; BD Biosciences, Franklin Lakes, NJ, USA) coatings were inserted into a 24-well culture plate.

For the migration assay, the HepG2 cells (100 μl, $5x10^4$) suspended in DMEM supplemented with 1% FBS were placed in the upper chamber and 0.5 ml CM collected from LX2-NRP-1 shRNA, LX2-NT shRNA and LX2-control was added into each lower chamber as a chemoattractant. The Transwell chambers were then incubated for 24 h.

For the invasion assay, 8-μm pore chamber inserts were coated with Matrigel. HepG2 cells in the log phase of growth were cultured in 6-well plates (100 μl; $5x10^5$/ml) in medium supplemented with 1% FBS for 24 h. The remaining steps were the same as for the migration assay. The Transwell chambers were incubated for 48 h.

The migrated and invaded cells on the underside of the filter were fixed in 37% methanol and stained with crystal violet (Boster Biological Technology, Pleasanton, CA, USA). Cell migration and invasion was determined by counting the stained cells in 10 randomly selected fields using a light microscope (magnification, x100).

ELISA. To detect the expression levels of soluble transforming growth factor (TGF)-β1 secreted by LX2 cells, $2x10^5$ LX2 cells with or without NRP-1 knockdown were seeded into 6-well plates, grown for 48 h and the supernatant was harvested for ELISA analysis. The human TGF-β1 Quantikine® ELISA kit from RapidBio Systems, Inc., (cat. no. DRE10098; Bedford, MA, USA) was used to perform ELISA TGF-β1 evaluation, according to the manufacturer's instructions. There were 6 replicates for each evaluation and the assessment was repeated three times.

In vivo experiments. Nude mice (n=24; age, 4 weeks; weight, 20±5 g; male:female, 1:1) were purchased from the Shanghai Experimental Animal Center (Shanghai, China). All nude mice were kept at the SPF level Laboratory Animal Center of Xi'an Jiaotong University (Xi'an, China). The housing conditions were as follows: Between 18 and 28˚C temperature, 50% relative humidity, 12/12 h lighr/dark cycle, 10 times/h of fresh air exchange, air flow speed <0.18 m/sec and noise <60 dB. The required water was acidified after high pressure disinfection (13). The food was treated with ultraviolet radiation. HepG2 cells ($1x10^6$) with or without LX2 ($2x10^5$) cell suspensions were injected subcutaneously into the armpits of nude mice to establish subcutaneous xenograft models without anesthesia to avoid affecting HepG2 cell proliferation. Tumor sizes were evaluated using calipers every 7 days. The size of PLC xenografts were evaluated using the following formula: Volume = AxB^2 x0.52 (A, length; B, width; all measurements were in millimeters). All nude mice were sacrificed after 4 weeks by decapitation following 5% isoflurane for induction of anesthesia and 1.5% isoflurane for the maintenance of anesthesia. The maximum tumor size was ~236 mm^3. The present study was approved by the Ethics Committee of Xi'an Jiaotong University.

Immunohistochemical (IHC) staining. IHC staining assays were performed according to the protocol described previously (14). Formalin-fixed and paraffin-embedded tissue samples were cut into 4-μm thick sections, deparaffinized with xylene and rehydrated in 100, 95, 90, 80 and 75% ethanol. Following washing in PBS, the tissue samples were boiled in antigen-retrieval buffer containing 0.01 M sodium citrate-hydrochloric acid (pH 6.0) for 15 min at 90-100˚C. The slides were rinsed with PBS and blocked overnight at 4˚C. Following three washes in PBS, the slides were incubated with a mouse monoclonal antibody directed against α-smooth muscle actin (α-SMA; 1:1,000; cat. no. EPR5368; Abcam, Cambridge, USA) at 4˚C overnight. Subsequently, the slides were incubated with a goat anti-rabbit immunoglobulin G (IgG; cat. no. E031320-01; EarthOx, LLC, San Francisco, CA, USA) antibody. The bound antibody was visualized using horseradish-peroxidase-streptavidin conjugates. The tissue sections were counterstained with hematoxylin, dehydrated in 75, 80, 90, 95, 80 and 100% ethanol and 99% xylene and then mounted and examined using a light microscope (CX31RTSF; magnification, x100; Olympus, Tokyo, Japan).

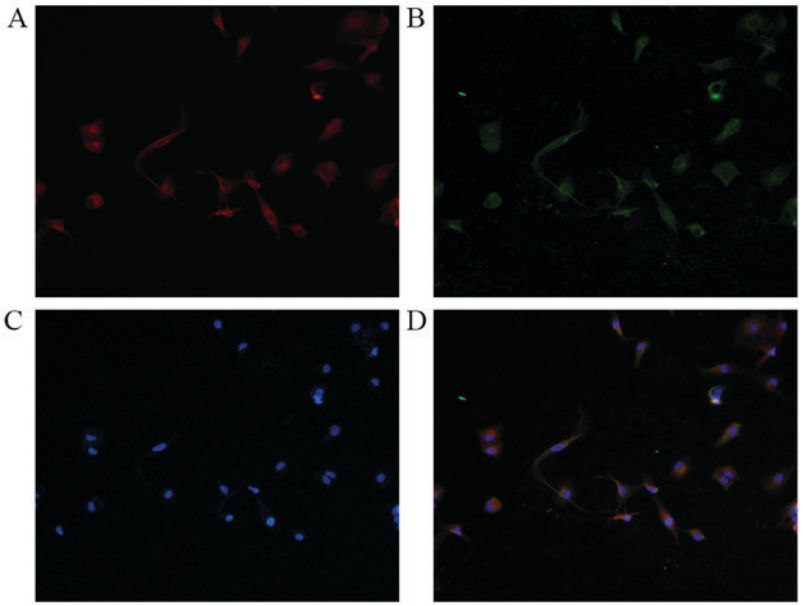

Figure 1. Immunofluorescent double-staining of LX2 cells. (A) Red fluorescence indicates NRP-1 expression; (B) green fluorescence indicates PDGFR-β expression; (C) DAPI-stained nuclei. (D) Merge: Yellow fluorescence indicates co-expression of NRP-1 and PDGFR-β. Magnification, x200. NRP-1, neuropilin-1; PDGFR-β, platelet-derived growth factor receptor-β.

Immunofluorescence staining. For fluorescent immunocytochemistry, the LX2 cells were fixed for 20 min in 4% paraformaldehyde in PBS, and the endogenous peroxidase activity was blocked using 3% hydrogen peroxide. The tissue samples were permeabilized with 0.3% Triton X-100 supplemented with 1% normal goat serum (ZSGB-BIO, Beijing, China) in PBS for 20 min on ice, pre-blocked for 30 min with bovine serum albumin (MP Biomedicals) at 37˚C and incubated with anti-Neuropilin-1 antibody (1:100; cat. no. EPR3113; Abcam) or anti-PDGFR-β (cat. no. sc-1627; Santa Cruz Biotechnology, Inc.) overnight at 4˚C. Staining was detected using fluorescein-conjugated secondary antibodies (Red Donkey anti-rabbit IgG, cat. no. A24421, and Green Donkey anti-goat IgG, cat. no. A24231 both from Abbkine, Inc., Redlands, CA, USA). Cell nuclei were counterstained with DAPI (1:1,000; Sigma-Aldrich; Merck KGaA). Slides were mounted and examined using a Nikon Corporation confocal microscope (magnification, x200) (Nikon Corporation, Tokyo, Japan).

Western blot analysis. The BCA assay kit (Shaanxi Pioneer Biotech Co., Ltd., Xi'an, China) was applied to detect protein concentrations. The LX2-NRP-1 shRNA, LX2-NT shRNA and LX2-control cells were lysed separately using cell lysis buffer (Shaanxi Pioneer Biotech Co., Ltd.) with protease inhibitors (Roche Diagnostics, Indianapolis, IN USA). Protein samples (10 μl) were electrophoretically resolved via denaturing SDS-PAGE and electro-transferred onto nitrocellulose membranes. The membranes were initially blocked with 5% non-fat dry milk in Tris-buffered saline for 2 h and subsequently probed with antibodies against NRP-1, extracellular signal-related kinase (ERK), phosphorylated-ERK and α-SMA. Following co-incubation with the primary antibodies at 4˚C overnight, the membranes were hybridized with the appropriate goat anti-mouse or anti-rabbit secondary antibody (Abcam) for 1 h at room temperature. The proteins were normalized to β-actin. The probed proteins were detected using enhanced chemiluminescence (EMD Millipore) and quantified by Image-pro plus 6.0 (Media Cybernetics, Rockville, MD, USA).

Statistical analysis. All data were analyzed using SPSS v.13.0 software (SPSS, Inc., Chicago, IL, USA). Data are presented as the mean ± standard deviation. Differences among the groups were compared with one-way ANOVA and the LSD-t test. Categorical data were compared with χ^2 tests. All statistical tests were two-tailed and $P<0.05$ was considered to indicate a statistically significant difference.

Results

NRP-1 expression level and its co-localization with platelet-derived growth factor receptor-β (PDGFR-β) in LX2 cells. Immunofluorescence double staining was performed for NRP-1 with PDGFR-β. As presented in Fig. 1, NRP-1 and PDGFR-β were detected on the surface of LX2 cells. The results confirmed that LX2 cells expressed NRP-1 and co-expressed with PDGFR-β in the cell membrane.

Viability of LX2 cells decreases following silencing of NRP-1 expression. The lentiviral-based shRNA transduction system is known to provide a high transduction rate and stable, long-term gene knockdown in HSCs (15). Western blot analysis verified that NRP-1 expression in LX2-NRP-1 shRNA cells was significantly low when compared with that in LX2-NT shRNA cells (Fig. 2A). MTT assays were performed to detect LX2 cell proliferation following the silencing of NRP-1. The results revealed that there were significant differences in the optical density at various time points (24, 48 and 72 h) between the LX2-NRP-1 shRNA and the LX2-NT shRNA groups (Fig. 2B). The expression of α-SMA is an important indicator of HSC activation; therefore, the present study compared the α-SMA

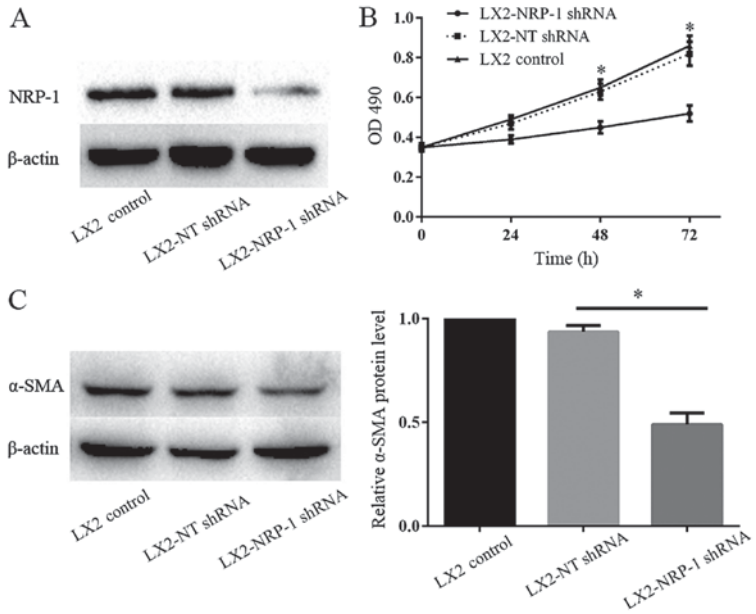

Figure 2. NRP-1 knockdown inhibits the viability and activation of LX2 cells. (A) NRP-1 shRNA efficiently knocked down NRP-1, as detected by western blotting; n=3. (B) MTT assay of LX2 optical density in various groups. n=3 repeats. (C) Western blot analysis revealed that the expression levels of α-SMA in LX2-NRP-1 shRNA cells were significantly lower compared with in LX2-NT shRNA cells; n=3. *P<0.05 by analysis of variance. NRP-1, neuropilin-1; shRNA, short hairpin RNA; α-SMA, α-smooth muscle actin; NT, non-targeting; OD, optical density.

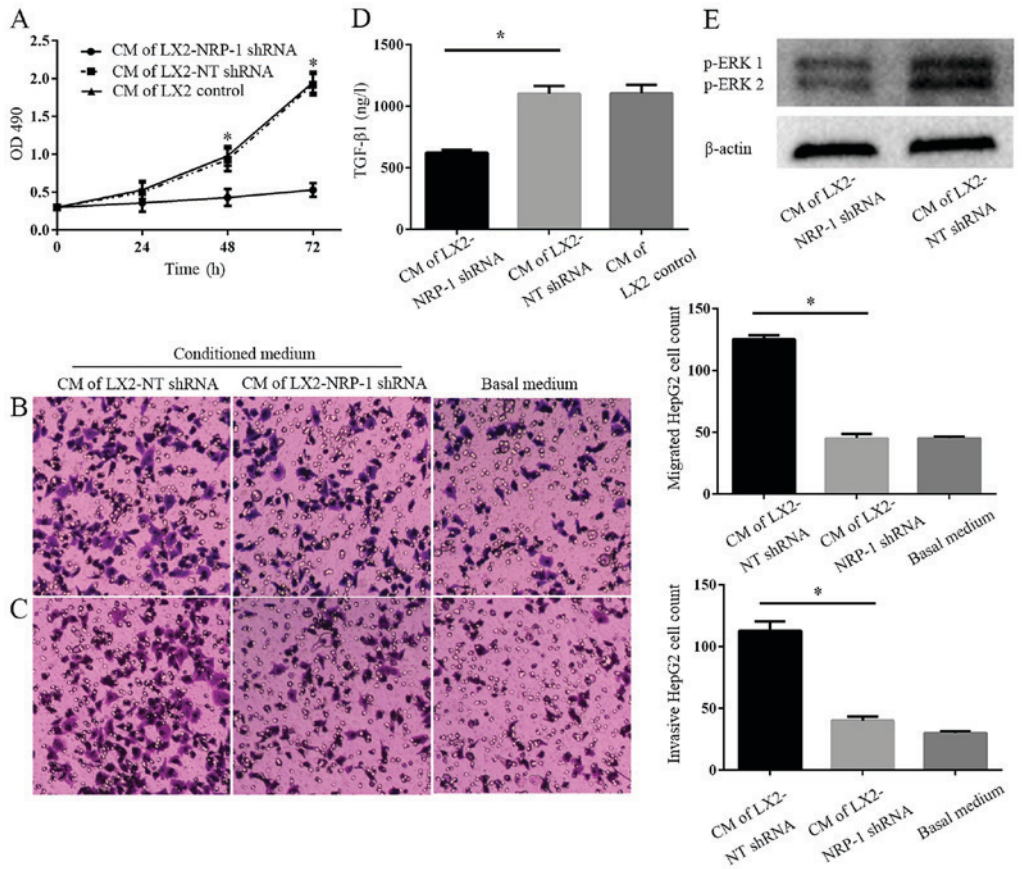

Figure 3. NRP-1 knockdown impairs the effects of LX2 cells on tumor proliferation, migration and invasion *in vitro*. (A) CM were collected from control LX2 cells (transduced with NT shRNA lentiviruses) and NRP-1 knockdown LX2 cells (transduced with NRP-1 shRNA lentiviruses). HepG2 cells cultured in LX2 cells CM were subjected to MTT assay analysis. CM of NRP-1 knockdown LX2 cells was less effective in promoting HepG2 proliferation compared with that of control LX2 cells. *P<0.05 by analysis of variance; n=3 repeats with similar results. CM described in (A) was used as the chemoattractant in the Transwell chamber assays. CM of NRP-1 knockdown LX2 cells was less effective at promoting HepG2 (B) migration and (C) invasion in comparison with that of control LX2 cells. *P<0.05 by analysis of variance; n=3 repeats (magnification, x100). (D) There was a markedly higher expression level of soluble TGF-β1 in CM from LX2-NT shRNA compared with LX2-NRP-1 shRNA CM (*P<0.05) as assessed by ELISA; n=3. (E) Western blot analysis using an antibody against phosphorylated ERK, p44 and p42, ERK1 and ERK2; n=3. CM, conditioned media; NT, non-targeting; shRNA, short hairpin RNA; NRP-1, neuropilin-1; ERK, extracellular signal-related kinase; OD, optical density; TGF-β1, transforming growth factor β1.

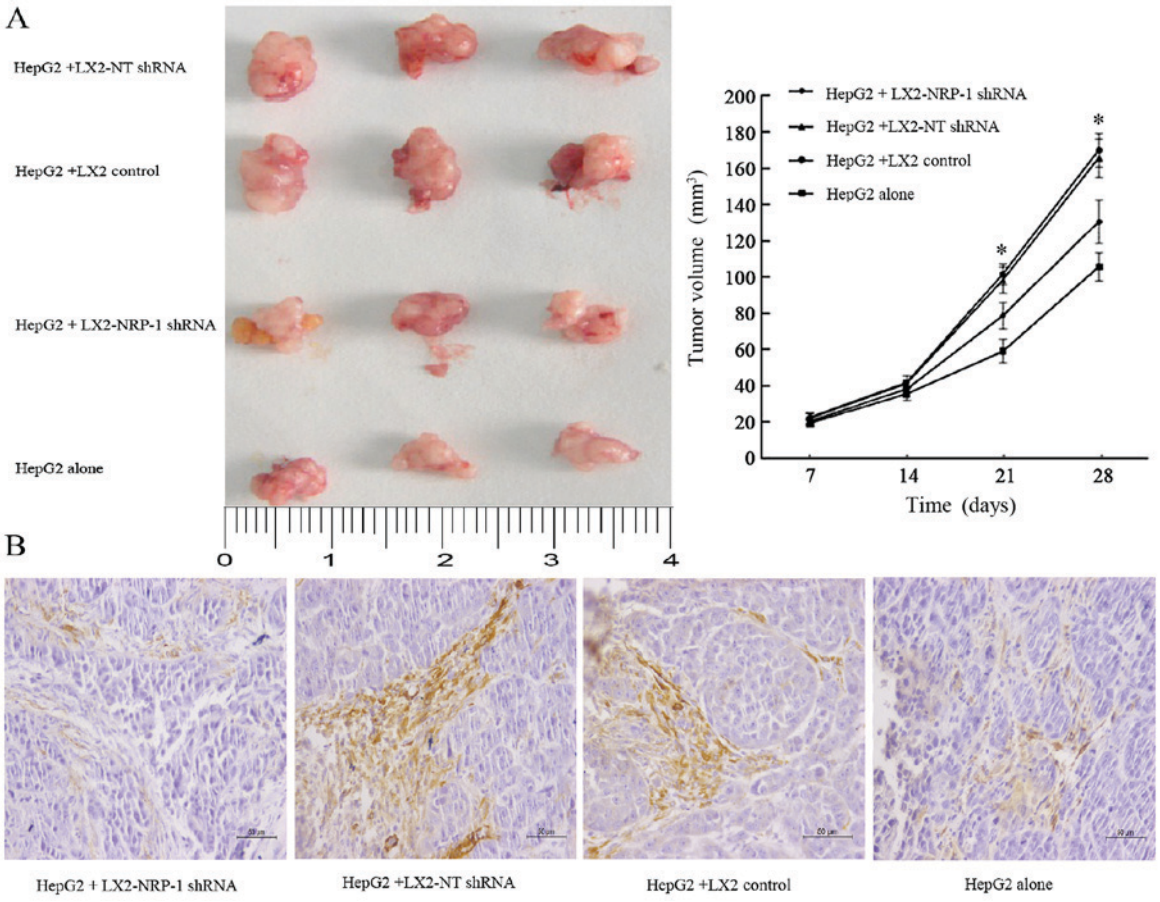

Figure 4. NRP-1 knockdown reduces stimulatory effects of LX2 cells on tumor growth *in vivo*. (A) HepG2 cells ($1x10^6$) mixed with NT or NRP-1 shRNA expressing LX2 cells ($2x10^5$) were implanted into nude mice by armpit injection. Tumor size was determined using a caliper. NRP-1 knockdown LX2 cells were less effective at promoting tumor growth in mice compared with control LX2 cells. The tumor was displayed in 4 cm scale. *P<0.05 by analysis of variance; n=24 tumors. (B) α-SMA staining of subcutaneous tumors in each group (magnification, x200). Scale bars, 50 μm. NT, non-targeting; NRP-1, neuropilin-1; shRNA, short hairpin RNA; α-SMA, α-smooth muscle actin.

protein expression levels in the control and NRP-1-knockdown LX2 cells using western blot analysis. As presented in Fig. 2C, the expression level of α-SMA in LX2-NRP-1 shRNA cells was significantly low when compare with in the LX2-NT shRNA cells. Thus, silencing NRP-1 expression in LX2 cells inhibited the activation of LX2 cells.

NRP-1 knockdown impairs the paracrine effects of LX2 cells on tumor cell proliferation, migration and invasion in vitro. CM from LX2-NRP-1 shRNA cells or LX2-NT shRNA cells was collected and used as a stimulant for tumor cells in the MTT and Transwell chamber assays. CM from the control and NRP-1 knockdown LX2 cells promoted HepG2 proliferation, migration and invasion *in vitro*, compared with the basal medium (Fig. 3A-C). However, CM of NRP-1 knockdown LX2 cells was less effective compared with that of the control LX2 cells (Fig. 3A-C). Therefore, the knockdown of NRP-1 impaired the effects of LX2 cells on the promotion of tumor cell proliferation, migration and invasion *in vitro*. To elucidate the potential molecular mechanisms underlying this process, an ELISA was performed and the results demonstrated there were markedly higher expression levels of soluble TGF-β1 in LX2-NT shRNA CM, as compared with in the CM from LX2-NRP-1 shRNA cells (Fig. 3D). Western blotting revealed that, compared with the LX2 and NRP-1 shRNA groups, CM from LX2-NT shRNA cells induced a high phosphorylation level of p42/p44 mitogen-activated protein kinases in HepG2 cells (Fig. 3E).

NRP-1 knockdown reduces the stimulatory effect of LX2 cells on tumor growth in mice. The present study co-implanted HepG2 and LX2 cells into mice in order to investigate whether NRP-1 in LX2 cells influenced tumor growth in mice. A mixture of HepG2 cells ($1x10^6$) and LX2 cells ($2x10^5$) cells expressing either NT shRNA or NRP-1 shRNA were implanted into nude mice via subcutaneous injection. Tumor growth curves revealed that control and NRP-1-knockdown LX2 cells promoted HepG2 tumor growth in mice (Fig. 4A). The average tumor size of NRP-1 knockdown LX2 cells was less than that of the control LX2 cells (Fig. 4A). Knockdown of NRP-1 attenuated the effect of LX2 cells with regard to promoting tumor growth in mice.

Expression of α-SMA weakens in xenograft tumors. IHC analysis of α-SMA, an established marker of activated HSC, revealed that the expression level of α-SMA in the stroma of tumors formed by the LX2-NRP-1 shRNA group were lower compared with in the LX2-NT shRNA and the LX2 control group, whereas the expression was low or absent in the HepG2 alone group (Fig. 4B).

Discussion

HCC is the most common type of primary tumor in the liver (16). Although advances have been made regarding the cellular and molecular mechanisms underlying liver carcinogenesis, PLC has one of the highest mortality rates worldwide; therefore, the development of innovative therapeutic options is required. An increasing number of studies have highlighted the crucial role of the tumor microenvironment in the pathogenesis of cancer. Thus, targeting the tumor microenvironment is now viewed as a promising therapeutic strategy for treating cancer in a variety of organs, including the liver (17,18). As an important stromal cell type in the liver tumor environment, HSCs may represent attractive targets in the design of innovative therapeutic strategies against liver carcinogenesis.

It has previously been reported that PDGF, the strongest cytokine promoting HSC activation, may bind with its receptor, PDGFR-β, and promote HSC activation, whereas NRP-1 contributes to the promotion of PDGF-mediated activation of HSCs (11). The present study revealed that NRP-1 was expressed on the membrane of LX2 cells and co-localized with PDGFR-β. Furthermore, it was demonstrated that silencing of NRP-1 expression of LX2 cells inhibited the proliferation and α-SMA expression levels of LX2 cells, thus the activation of LX2 cells was inhibited.

HSC promotion of the proliferation, migration and invasion of PLC cells relies on the mechanisms underlying activated HSC-mediated transformation into myofibroblasts, which secrete large amounts of cytokines, extracellular matrix proteins and integrin-metalloproteinase-9 (ADAM9) (19). These factors include TGF-β, PDGF, hepatocyte growth factor, stromal cell-derived factor-1 and ADAM9, which are able to promote the proliferation of and trigger epithelial-mesenchymal transition in PLC cells, resulting in the enhancement of cell migration and invasion (20,21). In the present study, following NRP-1 expression silencing, the effect of LX2 cells on the promotion of HepG2 cell proliferation was reduced. Similarly, the effect of CM on promoting the migration and invasion of HepG2 cells was also significantly reduced. Therefore, the present study suggested that the attenuated effects of HepG2 cell proliferation, migration and invasion may be attributed to the reduction in cytokines and matrix components in the CM. Subsequently, the present study performed an ELISA and revealed that the expression of TGF-β1 protein in LX2-NT shRNA CM was increased compared with that in LX2-NRP-1 shRNA CM. The present study suggested that combinations of these factors, and others factors not discussed herein, that are secreted by activated HSCs may induce the tumorigenic effects on HepG2 cells observed in the present and prior study (22).

In addition to the soluble factors released by activated HSC, further mechanisms may be involved in the observed carcinogenic effects. For example, Coulouarn and Clément (23) revealed that HSCs affect the progression and metastasis of hepatic tumors through extracellular matrix remodeling. A previous study investigating other types of tumors demonstrated that tumor cells further induced the expression of tumorigenic factors via activated HSCs, indicating a mutual interaction of cancer cells and stromal myofibroblasts in the promotion of carcinogenesis (24).

As a potential molecular mechanism underlying the effect of LX2 cells on HepG2 cells, the present study identified that the activity of ERK in HepG2 cells induced by CM collected from LX2-NRP-1 shRNA cells was decreased as compared with the LX2-NT shRNA. It has previously been demonstrated that aberrant activation of the mitogen activated protein kinase/ERK signaling pathway was involved in the progression of human PLC (25). Increased ERK activation is known to induce HCC cell proliferation and to protect HCC cells from apoptosis (26). Furthermore, increased ERK activity has been revealed to affect the migratory activity and invasiveness of HCC cells, suggesting that this molecular pathway may be critical in the intrahepatic metastasis of HCC (27).

In vivo experiments confirmed that HSCs promotes the growth of PLC and that this effect was attenuated following NRP-1 expression silencing. Subsequent analysis of the interaction between HSCs and HepG2 cells *in vivo* demonstrated α-SMA expression levels in the LX2-NRP-1 shRNA group were lower compared with in the LX2-NT shRNA and LX2 control groups, whereas the expression levels were low or absent in the HepG2 alone group. This finding indicated that the activation of LX2 cells was altered and α-SMA expression was downregulated following NRP-1 expression silencing, which was consistent with the results of the *in vitro* experiments.

The HepG2 cell line was used to investigate primary liver cancer in this study, it was originally thought to be a hepatocellular carcinoma cell line but has been revealed to derive from hepatoblastoma (28). However, it is a suitable *in vitro* and *in vivo* model for the study of hepatocarcinogenesis, and such misidentification is unlikely to affect the outcome of the study.

To conclude, the present study observed NRP-1 expression in and confirmed the co-localization of NRP-1 and PDGFR-β in LX2 cells. Following silencing of NRP-1 expression in LX2 cells, the activation of LX2 cells was inhibited, and the effect on the promotion of proliferation, migration and invasion of HepG2 cells was reduced. Finally, *in vivo* experiments demonstrated that silencing NRP-1 expression in HSCs may attenuate the growth of PLC, highlighting the contribution of NRP-1 as a potential target for PLC therapy.

Acknowledgements

The present study was supported by the National Natural Science Foundation of China (grant no. 81572420).

References

1. Torre LA, Bray F, Siegel RL, Ferlay J, Lortet-Tieulent J and Jemal A: Global cancer statistics. CA Cancer J Clin 65: 87-108, 2015.
2. Albini A and Sporn MB: The tumour microenvironment as a target for chemoprevention. Nat Rev Cancer 7: 139-147, 2007.
3. Yan XL, Fu CJ, Chen L, Qin JH, Zeng Q, Yuan HF, Nan X, Chen HX, Zhou JN, Lin YL, *et al*: Mesenchymal stem cells from primary breast cancer tissue promote cancer proliferation and enhance mammosphere formation partially via EGF/EGFR/Akt pathway. Breast Cancer Res Treat 132: 153-164, 2012.
4. Coulouarn C, Corlu A, Glaise D, Guénon I, Thorgeirsson SS and Clément B: Hepatocyte-stellate cell cross-talk in the liver engenders a permissive inflammatory microenvironment that drives progression in hepatocellular carcinoma. Cancer Res 72: 2533-2542, 2012.
5. van Zijl F, Mair M, Csiszar A, Schneller D, Zulehner G, Huber H, Eferl R, Beug H, Dolznig H and Mikulits W: Hepatic tumor-stroma crosstalk guides epithelial to mesenchymal transition at the tumor edge. Oncogene 28: 4022-4033, 2009.

6. Amann T, Bataille F, Spruss T, Mühlbauer M, Gäbele E, Schölmerich J, Kiefer P, Bosserhoff AK and Hellerbrand C: Activated hepatic stellate cells promote tumorigenicity of hepatocellular carcinoma. Cancer Sci 100: 646-653, 2009.
7. Kolodkin AL, Levengood DV, Rowe EG, Tai YT, Giger RJ and Ginty DD: Neuropilin is a semaphorin III receptor. Cell 90: 753-762, 1997.
8. Soker S, Takashima S, Miao HQ, Neufeld G and Klagsbrun M: Neuropilin-1 is expressed by endothelial and tumor cells as an isoform-specific receptor for vascular endothelial growth factor. Cell 92: 735-745, 1998.
9. Pellet-Many C, Frankel P, Jia H and Zachary I: Neuropilins: Structure, function and role in disease. Biochem J 411: 211-226, 2008.
10. Zachary IC, Frankel P, Evans IM and Pellet-Many C: The role of neuropilins in cell signalling. Biochem Soc Trans 37: 1171-1178, 2009.
11. Cao S, Yaqoob U, Das A, Shergill U, Jagavelu K, Huebert RC, Routray C, Abdelmoneim S, Vasdev M, Leof E, *et al*: Neuropilin-1 promotes cirrhosis of the rodent and human liver by enhancing PDGF/TGF-beta signaling in hepatic stellate cells. J Clin Invest 120: 2379-2394, 2010.
12. Zheng JB, Geng ZM, Chen Q and Wang L: Construction of recombinant lentiviral vector containing shRNA for human neuropilin-1 gene. Xi Bao Yu Fen Zi Mian Yi Xue Za Zhi 28: 1200-1203, 2012 (In Chinese).
13. Tusnio A, Taciak M, Barszcz M, Paradziej-Łukowicz J, Olędzka I, Wiczkowski W, Szumska M and Skomiał J: Thermal sterilization affects the content of selected compounds in diets for laboratory animals. J Anim Feed Sci 23: 351-360, 2014.
14. Chen C, Shen H, Tao J, Song H, Ma L, Wang L and Geng Z: Effect of cancer-associated fibroblasts on proliferation and invasion of gallbladder carcinoma cells. Nan Fang Yi Ke Da Xue Xue Bao 35: 1149-1154, 2015 (In Chinese).
15. Liu C, Billadeau DD, Abdelhakim H, Leof E, Kaibuchi K, Bernabeu C, Bloom GS, Yang L, Boardman L, Shah VH and Kang N: IQGAP1 suppresses TβRII-mediated myofibroblastic activation and metastatic growth in liver. J Clin Invest 123: 1138-1156, 2013.
16. Omata M, Lesmana LA, Tateishi R, Chen PJ, Lin SM, Yoshida H, Kudo M, Lee JM, Choi BI, Poon RT, *et al*: Asian pacific association for the study of the liver consensus recommendations on hepatocellular carcinoma. Hepatol Int 4: 439-474, 2010.
17. Junttila MR and de Sauvage FJ: Influence of tumour micro-environment heterogeneity on therapeutic response. Nature 501: 346-354, 2013.
18. Hernandez-Gea V, Toffanin S, Friedman SL and Llovet JM: Role of the microenvironment in the pathogenesis and treatment of hepatocellular carcinoma. Gastroenterology 144: 512-527, 2013.
19. Carloni V, Luong TV and Rombouts K: Hepatic stellate cells and extracellular matrix in hepatocellular carcinoma: More complicated than ever. Liver Int 34: 834-843, 2014.
20. Mikula M, Proell V, Fischer AN and Mikulits W: Activated hepatic stellate cells induce tumor progression of neoplastic hepatocytes in a TGF-beta dependent fashion. J Cell Physiol 209: 560-567, 2006.
21. Fischer AN, Fuchs E, Mikula M, Huber H, Beug H and Mikulits W: PDGF essentially links TGF-beta signaling to nuclear beta-catenin accumulation in hepatocellular carcinoma progression. Oncogene 26: 3395-3405, 2007.
22. Gupta DK, Singh N and Sahu DK: TGF-β mediated crosstalk between malignant hepatocyte and tumor microenvironment in hepatocellular carcinoma. Cancer Growth Metastasis 7: 1-8, 2014.
23. Coulouarn C and Clément B: Stellate cells and the development of liver cancer: Therapeutic potential of targeting the stroma. J Hepatol 60: 1306-1309, 2014.
24. Lu Y, Lin N, Chen Z and Xu R: Hypoxia-induced secretion of platelet-derived growth factor-BB by hepatocellular carcinoma cells increases activated hepatic stellate cell proliferation, migration and expression of vascular endothelial growth factor-A. Mol Med Rep 11: 691-697, 2015.
25. Min L, He B and Hui L: Mitogen-activated protein kinases in hepatocellular carcinoma development. Semin Cancer Biol 21: 10-20, 2011.
26. Takeishi K, Taketomi A, Shirabe K, Toshima T, Motomura T, Ikegami T, Yoshizumi T, Sakane F and Maehara Y: Diacylglycerol kinase alpha enhances hepatocellular carcinoma progression by activation of Ras-Raf-MEK-ERK pathway. J Hepatol 57: 77-83, 2012.
27. Chan LK, Chiu YT, Sze KM and Ng IO: Tensin4 is up-regulated by EGF-induced ERK1/2 activity and promotes cell proliferation and migration in hepatocellular carcinoma. Oncotarget 6: 20964-20976, 2015.
28. López-Terrada D, Cheung SW, Finegold MJ and Knowles BB: Hep G2 is a hepatoblastoma-derived cell line. Hum Pathol 40: 1512-1515, 2009.